Published in final edited form as:
J Biomech Eng. 2010 November ; 132(11): 111004. doi:10.1115/1.4002588.

Anisotropic Hydraulic Permeability Under Finite Deformation

Gerard A. Ateshian[1] and **Jeffrey A. Weiss**[2]

[1] Department of Mechanical Engineering, Columbia University, New York

[2] Departments of Bioengineering and Orthopedics, University of Utah, Salt Lake City

Abstract

The structural organization of biological tissues and cells often produces anisotropic transport properties. These tissues may also undergo large deformations under normal function, potentially inducing further anisotropy. A general framework for formulating constitutive relations for anisotropic transport properties under finite deformation is lacking in the literature. This study presents an approach based on representation theorems for symmetric tensor-valued functions and provides conditions to enforce positive semi-definiteness of the permeability or diffusivity tensor. Formulations are presented which describe materials that are orthotropic, transversely isotropic, or isotropic in the reference state, and where large strains induce greater anisotropy. Strain-induced anisotropy of the permeability of a solid-fluid mixture is illustrated for finite torsion of a cylinder subjected to axial permeation. It is shown that, in general, torsion can produce a helical flow pattern, rather than the rectilinear pattern observed when adopting a more specialized, unconditionally isotropic spatial permeability tensor commonly used in biomechanics. The general formulation presented in this study can produce both affine and non-affine reorientation of the preferred directions of material symmetry with strain, depending on the choice of material functions. This study addresses a need in the biomechanics literature by providing guidelines and formulations for anisotropic strain-dependent transport properties in porous-deformable media undergoing large deformations.

Introduction

Biological soft tissues can be described as mixtures of a solid matrix and an interstitial fluid. If the solid matrix exhibits structural anisotropy, the transport properties of the fluid through the solid matrix may also be anisotropic [1, 2]. For example, for a collagenous tissue that exhibits preferred fiber orientations, permeability of the solvent or diffusivity of the solutes in the directions parallel and perpendicular to the fibers may have different values [3–10]. Therefore, in general, transport properties are formulated in tensorial form, such as the permeability or diffusivity tensors.

When tissues undergo finite deformation, the material symmetry in the deformed configuration may be different than the material symmetry in the reference configuration. A material that exhibits isotropic transport properties in the reference configuration may develop strain-induced anisotropy under finite deformation. To the best of our knowledge, a general approach for formulating anisotropic properties for the permeability tensor while accounting for the possibility of strain-induced anisotropy under finite deformation has not been presented previously. Such a formulation must take into account that the permeability tensor is symmetric and positive definite. This study presents a general approach based on representation theorems for symmetric tensor-valued functions [11, 12].

Formulation

Permeability Tensor

The permeability tensor describes frictional interactions between a porous solid matrix and its interstitial fluid. From the equation of conservation of linear momentum for the fluid, when the effects of viscosity are neglected relative to the effects of permeability, under quasi-static conditions and in the absence of external body forces, the basic relation for the flux of interstitial fluid relative to the solid is

$$\mathbf{w} = -\mathbf{k} \cdot \operatorname{grad} p, \tag{1}$$

where **w** is the relative fluid flux, **k** is the second-order hydraulic permeability tensor, and p is the interstitial fluid pressure. Based on the second law of thermodynamics, **k** must be symmetric and positive semi-definite (see Appendix).

Material and Spatial Frames

The relation of Eq.(1) is given in the spatial configuration, therefore **k** represents the spatial permeability tensor. The corresponding permeability tensor in the material frame is obtained using the standard Piola transformation [13]:

$$\mathbf{K} = J\mathbf{F}^{-1} \cdot \mathbf{k} \cdot \mathbf{F}^{-T}, \tag{2}$$

where **F** is the deformation gradient for the solid matrix. Equivalently,

$$\mathbf{k} = J^{-1}\mathbf{F} \cdot \mathbf{K} \cdot \mathbf{F}^{T} \tag{3}$$

recovers the permeability tensor in the spatial frame [14].

In a nonlinear finite element implementation of mixture analysis under finite strain, it is necessary to evaluate the linearization of the permeability tensor along increments $\Delta\mathbf{u}$ in the solid matrix displacement:

$$D\mathbf{K}[\Delta\mathbf{u}] = \mathbb{K} : \frac{1}{2} D\mathbf{C}[\Delta\mathbf{u}], \tag{4}$$

where $\mathbf{C} = \mathbf{F}^{T} \cdot \mathbf{F}$ is the right Cauchy-Green tensor, D is the directional derivative operator [13],[1] and

$$\mathbb{K} = 2\frac{\partial \mathbf{K}}{\partial \mathbf{C}} \tag{5}$$

---

[1] $Df(\mathbf{x})[\mathbf{u}] = \left.\frac{d}{d\varepsilon}\right|_{\varepsilon=0} f(\mathbf{x}+\varepsilon\mathbf{u})$ for any function $f(\mathbf{x})$.

is a fourth-order tensor representing the rate of change of **K** with strain, in the material frame. The corresponding tensor in the spatial frame is obtained using the Piola transformation for fourth-order tensors, 2

$$\mathbb{k}=J^{-1}(\mathbf{F}\underline{\otimes}\mathbf{F}):\mathbb{K}:(\mathbf{F}^T\underline{\otimes}\mathbf{F}^T). \tag{6}$$

Based on the relations of Eqs.(5)–(6) and the symmetry of **K** and **C** , $\mathbb{k}$ and $\mathbb{K}$ exhibit minor symmetries (for example, $k_{ijkl} = k_{jikl}$ and $k_{ijkl} = k_{ijlk}$) but not necessarily major symmetry ($\mathbb{k} \neq \mathbb{k}^T$, or equivalently $k_{ijkl} \neq k_{klij}$).

Constraints on Constitutive Relations

The dependence of the permeability tensor on the deformation of the porous solid matrix must be specified via a constitutive relation. Except for the requirements of symmetry and positive semi-definiteness, there are no other formal thermodynamic constraints on this formulation. However, the permeability should reduce to zero in the limit of pore closure, in order to properly produce zero fluid flux according to Eq.(1). Let the solid and fluid volume fractions be given by ϕ^s and ϕ^f , respectively. The mixture saturation condition (the absence of voids) may be represented by

$$\phi^s+\phi^f=1. \tag{7}$$

When each constituent is intrinsically incompressible, the conservation of mass for the porous solid matrix implies that

$$\phi^s=\phi_r^s/J, \tag{8}$$

where ϕ_r^s is the solid volume fraction in the reference state ($\mathbf{C} = \mathbf{I}$).

In the analysis of saturated solid-fluid mixtures, pore closure occurs when all the fluid has been squeezed out of the $\phi^f = 0$ and $\phi^s = 1$, implying that $J=\phi_r^s$ at pore closure. Therefore, an additional constraint that may be placed on constitutive relations for the permeability tensor is the requirement that it reduces to zero in the limit of pore closure,

$$\lim_{J\to\phi_r^s}\mathbf{K}=\mathbf{0}, \qquad \lim_{J\to\phi_r^s}\mathbf{k}=\mathbf{0}. \tag{9}$$

Representation Theorem for Tensor-Valued Functions

This study seeks to formulate a framework for constitutive modeling of the permeability tensor, which is a second-order symmetric tensor function of the strain. A general approach is sought, which can subsequently be specialized to account for various constraints specific to the permeability tensor. Therefore, the formulation starts from basic principles embodied in representation theorems for symmetric tensor-valued functions [11, 12]. These representation theorems can be formulated for various postulated material symmetries,

---

[2]The tensor product $\otimes$ between second-order tensors **A** and **B** is defined by $(\mathbf{A}\otimes\mathbf{B})_{ijkl} = A_{ik}B_{jl}$ in a Cartesian basis [15].

though the literature generally describes representations for orthotropic and higher symmetries. Therefore, the presentation starts with materials whose transport properties are orthotropic, then proceeds to higher symmetries, including isotropy and transverse isotropy.

Orthotropy—An orthotropic material has three orthogonal planes of symmetry. Let the vectors $\mathbf{A}_a$ represent the unit normal vectors to these planes in the material frame (a = 1,2,3). Then, according to the representation theorem for orthotropic symmetric tensor-valued functions [11, 12, 16], the functional dependency of the permeability tensor in the material frame is given by $\mathbf{K}(\mathbf{A}_1, \mathbf{A}_2, \mathbf{A}_3, \mathbf{C})$, where $\mathbf{A}_a \cdot \mathbf{A}_b = \boldsymbol{\delta}_{ab}$ (Kronecker delta), and the most general dependence on strain is given by

$$\mathbf{K}=K_0\mathbf{C}^{-1}+\sum_{a=1}^{3}K_1^a\mathbf{M}_a+K_2^a(\mathbf{M}_a\cdot\mathbf{C}+\mathbf{C}\cdot\mathbf{M}_a),\qquad \mathbf{M}_a=\mathbf{A}_a\otimes\mathbf{A}_a,\tag{10}$$

where the scalars K_0, K_1^a and K_2^a are functions of the following strain invariants:

$$I_3=\det\mathbf{C},\qquad I_{a+3}=\mathbf{M}_a:\mathbf{C},\qquad I_{a+6}=\mathbf{M}_a:\mathbf{C}^2,\qquad a=1,2,3.\tag{11}$$

$\mathbf{C}$ and $\mathbf{C}^{-1}$ are positive definite for any arbitrary state of strain (their eigenvalues are always positive); based on its definition, $\mathbf{M}_a$ is similarly a positive semi-definite tensor. Since the sum of positive definite tensors produces a positive definite tensor [17], to ensure that $\mathbf{K}$ is positive semi-definite for any arbitrary state of strain, it is necessary and sufficient to formulate the scalar functions K_i such that

$$K_i(I_j)\geq 0,\qquad \forall I_j,\ j=3,\cdots,9.\tag{12}$$

In this expression, K_i is used generically to represent K_0, K_1^a and K_2^a. These constraints are thus specific to the constraint of positive semi-definiteness for the permeability tensor. In addition, to satisfy the constraint of Eq.(9), it is necessary and sufficient to satisfy

$$\lim_{J\to\phi_r^s}K_i=0,\tag{13}$$

Where $J=\sqrt{I_3}$.

Using Eq.(3), the permeability tensor in the spatial frame is given by

$$\mathbf{k}=k_0\mathbf{I}+\sum_{a=1}^{3}k_1^a\mathbf{m}_a+k_2^a(\mathbf{m}_a\cdot\mathbf{b}+\mathbf{b}\cdot\mathbf{m}_a),\qquad \mathbf{m}_a=\mathbf{F}\cdot\mathbf{M}_a\cdot\mathbf{F}^T,\tag{14}$$

where

$$k_0=J^{-1}K_0, \quad k_1^a=J^{-1}K_1^a, \quad k_2^a=J^{-1}K_2^a. \tag{15}$$

The derivative of **K** with respect to the strain may be obtained from Eq.(5) using the chain rule of differentiation,3

$$\mathbb{K}=\mathbf{C}^{-1}\otimes\widehat{\mathbf{K}}_0-2K_0\mathbf{C}^{-1}\underline{\bar{\otimes}}\mathbf{C}^{-1}+\sum_{a=1}^{3}\mathbf{M}_a\otimes\widehat{\mathbf{K}}_1^a+\sum_{a=1}^{3}(\mathbf{M}_a\cdot\mathbf{C}+\mathbf{C}\cdot\mathbf{M}_a)\otimes\widehat{\mathbf{K}}_2^a+2K_2^a(\mathbf{M}_a\underline{\bar{\otimes}}\mathbf{I}+\mathbf{I}\underline{\bar{\otimes}}\mathbf{M}_a), \tag{16}$$

where

$$\widehat{\mathbf{K}}_i=2\frac{\partial K_i}{\partial \mathbf{C}}=2\left[I_3\frac{\partial K_i}{\partial I_3}\mathbf{C}^{-1}+\sum_{b=1}^{3}\frac{\partial K_i}{\partial I_{b+3}}\mathbf{M}_b+\frac{\partial K_i}{\partial I_{b+6}}(\mathbf{M}_b\cdot\mathbf{C}+\mathbf{C}\cdot\mathbf{M}_b)\right]. \tag{17}$$

In this expression, $\hat{\mathbf{K}}_i$ is used generically to represent $\hat{\mathbf{K}}_0$, $\widehat{\mathbf{K}}_1^a$ and $\widehat{\mathbf{K}}_2^a$. Using Eq.(6), the spatial representation of this fourth-order tensor becomes

$$\mathbb{k}=\mathbf{I}\otimes\widehat{\mathbf{k}}_0-2k_0\mathbf{I}\underline{\bar{\otimes}}\mathbf{I}+\sum_{a=1}^{3}\mathbf{m}_a\otimes\widehat{\mathbf{k}}_1^a+\sum_{a=1}^{3}(\mathbf{m}_a\cdot\mathbf{b}+\mathbf{b}\cdot\mathbf{m}_a)\otimes\widehat{\mathbf{k}}_2^a+2k_2^a(\mathbf{m}_a\underline{\bar{\otimes}}\mathbf{b}+\mathbf{b}\underline{\bar{\otimes}}\mathbf{m}_a), \tag{18}$$

where

$$\widehat{\mathbf{k}}_i=J^{-1}\mathbf{F}\cdot\widehat{\mathbf{K}}_i\cdot\mathbf{F}^T=2J^{-1}\left[I_3\frac{\partial K_i}{\partial I_3}\mathbf{I}+\sum_{b=1}^{3}\frac{\partial K_i}{\partial I_{b+3}}\mathbf{m}_b+\frac{\partial K_i}{\partial I_{b+6}}(\mathbf{m}_b\cdot\mathbf{b}+\mathbf{b}\cdot\mathbf{m}_b)\right]. \tag{19}$$

$\hat{\mathbf{k}}_i$ is used generically to represent $\hat{\mathbf{k}}_0$, $\widehat{\mathbf{k}}_1^a$ and $\widehat{\mathbf{k}}_2^a$.

Due to the symmetry of **I, C,** $\mathbf{C}^{-1}$ and $\mathbf{M}_a$, it follows from Eq.(16) that $\mathbb{K}$ satisfies the two minor symmetries, but not the major symmetry ($\mathbb{K}^T \neq \mathbb{K}$ in general); the same argument applies to $\mathbb{k}$.

Isotropy—The case of isotropy may be derived from the representation theorem for isotropic tensor-valued functions, or simply reduced from the orthotropic case presented above. For isotropic materials there is no preferred material direction, so that

$$K_1^a \equiv K_1, \quad K_2^a \equiv K_2, \quad a=1,2,3. \tag{20}$$

3The tensor products $\otimes$ and $\underline{\bar{\otimes}}$ between second-order tensors **A** and **B** are respectively defined by $(\mathbf{A}\otimes\mathbf{B})_{ijkl} = A_{ij}B_{kl}$ and $(\mathbf{A}\underline{\bar{\otimes}}\mathbf{B})_{ijkl}=\left(A_{ik}B_{jl}+A_{il}B_{jk}\right)/2$ in a Cartesian basis [15].

In this case, since $\sum_{a=1}^{3} \mathbf{M}_a = \mathbf{I}$ and

$$I_1 = \mathbf{I}:\mathbf{C} = \sum_{a=1}^{3} I_{a+3}, \qquad I_2 = \mathbf{I}:\mathbf{C}^2 = \sum_{a=1}^{3} I_{a+6}, \tag{21}$$

the permeability tensors in the material and spatial frames reduce to

$$\mathbf{K} = K_0 \mathbf{C}^{-1} + K_1 \mathbf{I} + 2K_2 \mathbf{C}, \tag{22}$$

$$\mathbf{k} = k_0 \mathbf{I} + k_1 \mathbf{b} + 2k_2 \mathbf{b}^2, \tag{23}$$

where all K_i's depend on I_1, I_2, I_3. The derivative of the material permeability tensor with respect to the strain becomes

$$\mathbb{K} = \mathbf{C}^{-1} \otimes \widehat{\mathbf{K}}_0 - 2K_0 \mathbf{C}^{-1} \underline{\bar{\otimes}} \mathbf{C}^{-1} + \mathbf{I} \otimes \widehat{\mathbf{K}}_1 + 2\mathbf{C} \otimes \widehat{\mathbf{K}}_2 + 4K_2 \mathbf{I} \underline{\bar{\otimes}} \mathbf{I}, \tag{24}$$

where

$$\widehat{\mathbf{K}}_i = 2\left(I_3 \frac{\partial K_i}{\partial I_3} \mathbf{C}^{-1} + \frac{\partial K_i}{\partial I_1} \mathbf{I} + 2\frac{\partial K_i}{\partial I_2} \mathbf{C} \right). \tag{25}$$

Similarly, for the spatial representation,

$$\mathbb{k} = \mathbf{I} \otimes \widehat{\mathbf{k}}_0 - 2k_0 \mathbf{I} \underline{\bar{\otimes}} \mathbf{I} + \mathbf{b} \otimes \widehat{\mathbf{k}}_1 + 2\mathbf{b}^2 \otimes \widehat{\mathbf{k}}_2 + 4k_2 \mathbf{b} \underline{\bar{\otimes}} \mathbf{b}, \tag{26}$$

where

$$\widehat{\mathbf{k}}_i = 2J^{-1}\left(I_3 \frac{\partial K_i}{\partial I_3} \mathbf{I} + \frac{\partial K_i}{\partial I_1} \mathbf{b} + 2\frac{\partial K_i}{\partial I_2} \mathbf{b}^2 \right). \tag{27}$$

Transverse Isotropy—The case of transverse isotropy may be similarly reduced from orthotropy by letting

$$K_j^1 = K_j^2 \equiv K_j^T, \qquad K_j^3 \equiv K_j^A, \qquad J = 1, 2, \tag{28}$$

where K_j^T and K_j^A represent permeability functions in the transverse plane of isotropy and along the axial direction normal to that plane, respectively. Then, the permeability tensors are given by

$$\mathbf{K}=K_0\mathbf{C}^{-1}+K_1^T\mathbf{I}+2K_2^T\mathbf{C}+\left(K_1^A-K_1^T\right)\mathbf{M}_3+\left(K_2^A-K_2^T\right)(\mathbf{M}_3\cdot\mathbf{C}+\mathbf{C}\cdot\mathbf{M}_3), \tag{29}$$

$$\mathbf{k}=k_0\mathbf{I}+k_1^T\mathbf{b}+2k_2^T\mathbf{b}^2+\left(k_1^A-k_1^T\right)\mathbf{m}_3+\left(k_2^A-k_2^T\right)(\mathbf{m}_3\cdot\mathbf{b}+\mathbf{b}\cdot\mathbf{m}_3), \tag{30}$$

where all K_i's are functions of I_1, I_2, I_3, I_6, I_9.4 Similarly,

$$\begin{aligned}\mathbb{K}=&\mathbf{C}^{-1}\otimes\widehat{\mathbf{K}}_0\\&-2K_0\mathbf{C}^{-1}\underline{\bar{\otimes}}\mathbf{C}^{-1}\\&+\mathbf{I}\otimes\widehat{\mathbf{K}}_1^T\\&+2\mathbf{C}\otimes\widehat{\mathbf{K}}_2^T\\&+4K_2^T\mathbf{I}\underline{\bar{\otimes}}\mathbf{I}\\&+\mathbf{M}_3\otimes\left(\widehat{\mathbf{K}}_1^A-\widehat{\mathbf{K}}_1^T\right)\\&+(\mathbf{M}_3\cdot\mathbf{C}\\&+\mathbf{C}\cdot\mathbf{M}_3)\otimes\left(\widehat{\mathbf{K}}_2^A-\widehat{\mathbf{K}}_2^T\right)+2\left(K_2^A-K_2^T\right)(\mathbf{M}_3\underline{\bar{\otimes}}\mathbf{I}\\&+\mathbf{I}\underline{\bar{\otimes}}\mathbf{M}_3),\end{aligned} \tag{31}$$

where

$$\widehat{\mathbf{K}}_i=2\left(I_3\frac{\partial K_i}{\partial I_3}\mathbf{C}^{-1}+\frac{\partial K_i}{\partial I_1}\mathbf{I}+2\frac{\partial K_i}{\partial I_2}\mathbf{C}+\frac{\partial K_i}{\partial I_6}\mathbf{M}_3+\frac{\partial K_i}{\partial I_9}(\mathbf{M}_3\cdot\mathbf{C}+\mathbf{C}\cdot\mathbf{M}_3)\right), \tag{32}$$

and

$$\mathbb{k}=\mathbf{I}\otimes\widehat{\mathbf{k}}_0-2k_0\mathbf{I}\underline{\bar{\otimes}}\mathbf{I}+\mathbf{b}\otimes\widehat{\mathbf{k}}_1^T+2\mathbf{b}^2\otimes\widehat{\mathbf{k}}_2^T+4k_2^T\mathbf{b}\underline{\bar{\otimes}}\mathbf{b}+\mathbf{m}_3\otimes\left(\widehat{\mathbf{k}}_1^A-\widehat{\mathbf{k}}_1^T\right)+(\mathbf{m}_3\cdot\mathbf{b}+\mathbf{b}\cdot\mathbf{m}_3)\otimes\left(\widehat{k}_2^A-\widehat{\mathbf{k}}_2^T\right)+2\left(k_2^A-k_2^T\right)(\mathbf{m}_3\underline{\bar{\otimes}}\mathbf{b}+\mathbf{b}\underline{\bar{\otimes}}\mathbf{m}_3), \tag{33}$$

where

4Conventionally, in a transversely isotropic formulation, the strain invariants $\mathbf{M}_3$: $\mathbf{C}$ and $\mathbf{M}_3$: $\mathbf{C}^2$ are denoted by I_4 and I_5, respectively. They appear as I_6 and I_9 in this treatment, to maintain a consistent notation between orthotropic and transversely isotropic formulations.

$$\widehat{\mathbf{k}}_i=2J^{-1}\left(I_3\frac{\partial K_i}{\partial I_3}\mathbf{I}+\frac{\partial K_i}{\partial I_1}\mathbf{b}+2\frac{\partial K_i}{\partial I_2}\mathbf{b}^2+\frac{\partial K_i}{\partial I_6}\mathbf{m}_3+\frac{\partial K_i}{\partial I_9}(\mathbf{m}_3\cdot\mathbf{b}+\mathbf{b}\cdot\mathbf{m}_3)\right). \tag{34}$$

Examples of Constitutive Relations

The most common constitutive relation for the hydraulic permeability tensor adopted in the biomechanics literature has the form

$$\mathbf{k}=k_0(J)\mathbf{I}, \tag{35}$$

where the specific dependence of k_0 on J is often an exponential or power-law function [18, 19], such as

$$k_0(J)=k_{0r}\left(\frac{J-\phi_r^s}{1-\phi_r^s}\right)^{\kappa_0}e^{M_0(J^2-1)/2}, \tag{36}$$

where k_{0r}, κ_0 and M_0 are material constants to be determined from experiments [18]. This function satisfies the constraints of Eqs.(12)–(13). This formulation represents a special case of permeability as given in Eq.(14), with $k_1^a=k_2^a=0$, which does not exhibit strain-induced anisotropy. Regardless of the state of strain in the material, $\mathbf{k}$ remains an isotropic tensor,5 implying that every plane through the material represents a plane of material symmetry for transport properties. It may be noted that this constitutive relation, formulated in the spatial frame, corresponds to $\mathbf{K} = K_0\mathbf{C}^{-1}$ in the material frame, where $K_0 = Jk_0$ as per Eq.(15). Thus, in the material frame, $\mathbf{K}$ is not an isotropic tensor for arbitrary states of strain.

For this special case of constitutive relation, the corresponding spatial form of the derivative with respect to strain reduces to

$$\mathbb{k}=k_0\left(\left[1+J\left(\frac{\kappa_0}{J-\phi_r^s}+M_0J\right)\right]\mathbf{I}\otimes\mathbf{I}-2\mathbf{I}\underline{\bar{\otimes}}\mathbf{I}\right). \tag{37}$$

Anisotropic permeability has generally been employed in problems with small deformations, for which the spatial and material representations are approximately the same. The most common choice of constitutive relation has had the form $\mathbf{K}=K_1^T\mathbf{I}+\left(K_1^A-K_1^T\right)\mathbf{M}_3$ for transverse isotropy [10, 20], or $\mathbf{K}=\sum_{a=1}^3 K_1^a\mathbf{M}_a$ for orthotropy [9, 21]. These formulations represent special cases of transversely isotropic permeability as given in Eq.(29) and orthotropic permeability as given in Eq.(10), with $K_0=K_2^a=0$ and K_1^a treated as constant.

Constitutive relations are guided by experimental measurements. Since permeation experiments in deformable tissues are challenging to perform, most permeation studies under finite deformation have been performed in one-dimensional setups, under unidirectional flow conditions [22, 23]. More often, material coefficients for an assumed

5A second-order tensor $\mathbf{T}$ is isotropic when $\mathbf{T} = \alpha\mathbf{I}$ for any scalar α.

permeability constitutive relation under finite deformation were obtained by curve-fitting the load-deformation response of soft tissues in confined compression [24–28]. Therefore, because of the one-dimensional nature of these finite deformation experiments, there is limited experimental data in the literature that can shed insight into the potential mechanism of strain-induced anisotropy in the permeability. Yet, even in the case of an isotropic material, the more general formulation for the spatial permeability given in Eq.(23) suggests that large deformations may induce an anisotropic permeability tensor, when either $k_1 \neq$ or $k_2 \neq 0$.

It is possible that the choices of permeability constitutive relations adopted for biological tissues to date represent special cases that do not necessarily explore the full range of possible deformation-induced responses. To explore the implications of strain-induced anisotropy in the permeability, consider the general case of Eq.(23), which represents the response for a material whose permeability is isotropic in a strain-free state ($\mathbf{b} = \mathbf{I}$). Under general deformations however ($\mathbf{b} \neq \mathbf{I}$), the permeability tensor is no longer an isotropic tensor. For arbitrary strain fields in an isotropic material, three planes of symmetry emerge which correspond to the principal planes of normal strain (the planes whose normals are the eigenvectors of $\mathbf{b}$). Therefore, in a material whose transport properties are isotropic under a strain-free state, strain-induced anisotropy produces orthotropic symmetry, with the orientation of the planes of symmetry varying with the state of strain.

If the permeability is anisotropic in a strain-free state, such as in the case of orthotropy, Eq. (14), it becomes evident that this anisotropy is manifested in the terms other than $k_0\mathbf{I}$ appearing in these general relations. Therefore, anisotropic transport properties can only be specified with material functions $k_1^a \neq 0$ or $k_2^a \neq 0$. In a strain-free state, the three planes of symmetry are normal to $\mathbf{V}_a$ (a = 1,2,3) by definition. However, under a general state of strain (when the eigenvectors of $\mathbf{b}$ do not align with $\mathbf{F}\cdot\mathbf{V}_a$), the strain-induced anisotropy degenerates to complete loss of symmetry (triclinic form). In effect, it is not possible to describe an orthotropic (or transversely isotropic, or monoclinic) spatial permeability tensor $\mathbf{k}$ whose planes of symmetry remain invariant with strain under general conditions.

For example, consider the special case of an orthotropic material where $k_0 = k_2^a = 0$, so that

$$\mathbf{k} = \sum_{a=1}^{3} k_1^a \mathbf{m}_a. \tag{38}$$

It should be evident that the strain-induced anisotropy for this special case obeys an affine transformation of the preferred material directions $\mathbf{A}_a$, since the expression for $\mathbf{m}_a$ in Eq. (14) may also be written as $\mathbf{m}_a = (\mathbf{F}\cdot\mathbf{A}_a) \otimes (\mathbf{F}\cdot\mathbf{A}_a)$. A constitutive form for k_1^a may be selected such that it produces the same permeability as the form of Eqs.(35)–(36) when considering the canonical problem of 1D permeation under finite deformation,

$$k_1^a(J) = \frac{k_{1r}^a}{J^2}\left(\frac{J - \phi_r^s}{1 - \phi_r^s}\right)^{\kappa_1^a} e^{M_1^a (J^2 - 1)/2}, \quad a = 1, 2, 3, \tag{39}$$

Where k_{1r}^a, κ_1^a and M_1^a represent material constants. The corresponding expression for $\mathbf{k}$ becomes

NIH-PA Author Manuscript
NIH-PA Author Manuscript

$$\mathbb{k}=\sum_{a=1}^{3}\left[J^2 M_1^a+\frac{J\left(\kappa_1^a-1\right)+\phi_r^s}{J-\phi_r^s}\right]k_1^a\mathbf{m}_a\otimes\mathbf{I}. \tag{40}$$

Another special case that may be considered here corresponds to $k_0=k_1^a=0$, such that

$$\mathbf{k}=\sum_{a=1}^{3}k_2^a(\mathbf{m}_a\cdot\mathbf{b}+\mathbf{b}\cdot\mathbf{m}_a) \tag{41}$$

For this choice, it is evident that the strain-induced anisotropy follows a non-affine transformation of the preferred material directions $\mathbf{A}_a$, since $\mathbf{m}_a\cdot\mathbf{b}+\mathbf{b}\cdot\mathbf{m}_a$ is neither equal nor proportional to $\mathbf{m}_a$. Once again, a constitutive form for k_2^a may be selected such that it produces the same permeability as the form of Eqs.(35)–(36) when considering the canonical problem of 1D permeation under finite deformation,

$$k_2^a(J)=\frac{k_{2r}^a}{2J^4}\left(\frac{J-\phi_r^s}{1-\phi_r^s}\right)^{\kappa_2^a}e^{M_2^a(J^2-1)/2},\ \ a=1,2,3. \tag{42}$$

The corresponding expression for $\mathbb{k}$ becomes

$$\mathbb{k}=\sum_{a=1}^{3}k_2^a\left[\left(J^2M_2^a+\frac{J\left(\kappa_2^a-3\right)+3\phi_r^s}{J-\phi_r^s}\right)(\mathbf{m}_a\cdot\mathbf{b}+\mathbf{b}\cdot\mathbf{m}_a)\otimes\mathbf{I}+2(\mathbf{m}_a\underline{\bar{\otimes}}\mathbf{b}+\mathbf{b}\underline{\bar{\otimes}}\mathbf{m}_a)\right] \tag{43}$$

These constitutive relations can be reduced to transverse isotropy and isotropy as shown above. Clearly, any number of specialized forms and combinations may be adopted for these constitutive relations. As a final example, for a referentially isotropic permeability tensor, a choice of constitutive relation may be given by

$$\mathbf{k}=\left(k_{0r}\mathbf{I}+\frac{k_{1r}}{J^2}\mathbf{b}+\frac{k_{2r}}{J^4}\mathbf{b}^2\right)\left(\frac{J-\phi_r^s}{1-\phi_r^s}\right)^{\kappa}e^{M(J^2-1)/2} \tag{44}$$

In this formulation, prescribing various values to k_{0r} , k_{1r} and k_{2r} can give preferential weight to affine or non-affine strain-induced anisotropy. In the canonical problems analyzed below, some salient features of strain-induced anisotropy are explored.

Canonical Problems

Isochoric Axial Stretch

Consider the isochoric axial stretch of an isotropic homogeneous cylinder,

$$[\mathbf{F}]=\begin{bmatrix} 1/\sqrt{\lambda} & 0 & 0 \\ 0 & 1/\sqrt{\lambda} & 0 \\ 0 & 0 & \lambda \end{bmatrix}, \tag{45}$$

for which $J = 1$ (no change in pore volume with deformation). The matrix of the permeability tensor resulting from Eq.(23) is

$$[\mathbf{k}]=\begin{bmatrix} k_0+\frac{k_1}{\lambda}+2\frac{k_2}{\lambda^2} & 0 & 0 \\ 0 & k_0+\frac{k_1}{\lambda}+2\frac{k_2}{\lambda^2} & 0 \\ 0 & 0 & k_0+k_1\lambda^2+2k_2\lambda^4 \end{bmatrix}. \tag{46}$$

As λ increases above unity with axial stretching, the radial and circumferential permeability components, $k_0 + k_1/\lambda + 2k_2/\lambda^2$,, will always be smaller than the axial component $k_0 + k_1\lambda^2 + k_2\lambda^4$, regardless of the functional dependence of k_i on I_j (j = 1,2,3). Thus, even though the pore volume does not change, the shape of the pores is altered with deformation such that the permeability tensor is no longer isotropic (unless $k_1 = k_2 = 0$); in this example, the symmetry reduces to transverse isotropy under axial stretching.

For example, consider that the isotropic permeability arises from a solid matrix consisting of randomly oriented fibers in the reference configuration, with each fiber orientation represented by the vector $\mathbf{N} = \sin\varphi\, \mathbf{e}_r + \cos\varphi\, \mathbf{e}_z$, $0\leq<\pi$. Assuming that fibers deform according to an affine transformation, they become oriented along

$$\mathbf{n}=\frac{\mathbf{F}\cdot\mathbf{N}}{|\mathbf{F}\cdot\mathbf{N}|}=\frac{\sin\varphi\,\mathbf{e}_r+\lambda^{3/2}\cos\varphi\,\mathbf{e}_z}{\sqrt{\lambda^3\cos^2\varphi+\sin^2\varphi}}. \tag{47}$$

As the axial stretch λ increases, the fibers turn toward the long axis of the cylinder, eventually lining up with $\mathbf{e}_z$ in the limit as $\lambda\to\infty$. Therefore, for this example of isochoric stretch of an isotropic material, according to Eq.(46), it is found that permeability becomes greater along the direction of preferred fiber reorientation than along the directions perpendicular to it.

The same conclusions would be reached for the case of confined axial stretch of a homogeneous isotropic cylinder, when $[\mathbf{F}]$ = diag $\{1,1,\lambda\}$.

Finite Torsion

In this example, a finite element analysis was used to illustrate strain-induced anisotropy in a biphasic isotropic cylinder subjected to torsion, with a pressure gradient applied axially to promote permeation. The finite element implementation of these formulations was incorporated into FEBio, an existing public-domain, open-source finite element program (http://mrl.sci.utah.edu/software?menu=Software). The cylinder had a diameter of 10 mm and was 25 mm long. Its solid matrix was described as a neo-Hookean isotropic elastic solid, with a Young's modulus of 1 MPa and Poisson's ratio set to zero. The permeability tensor was described by Eq.(44), where each of k_{0r} , k_{1r} and k_{2r} was respectively set to 10^3 mm^4/N·s, while the other two were set to zero. In all cases, the remaining material parameters were $\phi_r^s=0.2$, κ = 2, and $M = 0$. One end of the cylinder was constrained to have zero

NIH-PA Author Manuscript

NIH-PA Author Manuscript

displacements along all three coordinate directions, and a prescribed fluid pressure of 0.1 MPa. The other end was prescribed to rotate in its plane by a half-rotation (180° twist), and constrained to zero displacement along the axial direction; the fluid pressure was also constrained to zero on this face (free-draining conditions). The lateral surface was traction-free and impermeable.

The steady-state response was examined here, since the focus of this analysis was on the effect of strain-induced anisotropy on the relative fluid flux **w** , rather than the transient response to the applied boundary conditions.

Results showed that the streamlines of solvent volume flux remained rectilinear in the case of $\mathbf{k} = k_0\mathbf{I}$ ($k_{0r} \neq 0$ $k_{1r} = k_{2r} = 0$), regardless of the applied deformation (Figure 1c). For the other two cases however, the flux twisted into a helical pattern with torsion (Figure 1d). A closer examination of the flux pattern, when superposed on the deformed finite element mesh, confirmed that the case $\mathbf{k} = k_1\mathbf{b}$ produced an affine transformation, with the flux aligning exactly with the deformed mesh (Figure 2c). In contrast, for the case $\mathbf{k} = 2k_2\mathbf{b}^2$, the flux vector twisted further than the direction prescribed by an affine transformation (Figure 2d).

Discussion

This study proposed a systematic approach for formulating constitutive relations for the anisotropic, strain-dependent hydraulic permeability tensor in deformable porous media. The hydraulic permeability is a material function that relates the flux of interstitial fluid to the pressure gradient, Eq.(1). A primary motivation for this aim was the observation that many biological tissues undergo large deformations during normal function, yet few guidelines are currently available in the literature for formulating strain-dependent anisotropic transport properties under such deformations.

The first step was to recognize the constraints imposed by the entropy inequality on the permeability tensor, which must be symmetric and positive semi-definite. This was followed by the recognition that the fourth-order tensor representing the rate of change of the permeability tensor with strain must satisfy minor symmetries but need not exhibit major symmetry.

Using the framework of representation theorems for symmetric tensor-valued functions, general expressions were provided for orthotropic, isotropic and transversely isotropic permeability tensors. These tensor functions are dependent on scalar functions of the strain invariants, $ki\,(I_j) = J^{-1}\,K_i\,(I_j)$, which, when positive for arbitrary strains, enforce positive-definiteness of the permeability tensor.

These general formulations demonstrated that, in general, strain induces anisotropy in the permeability tensor under finite deformation, even if the permeability tensor was isotropic in the reference configuration. Thus, the most commonly used permeability constitutive relation under finite deformation in soft tissue mechanics, Eq.(35) [14, 24, 29–37], was shown to represent only a special case where permeability in the spatial frame remains isotropic regardless of the state of strain. Whether the permeability of soft tissues should obey Eq.(35) or a more general form that results in strain-induced anisotropy, such as Eq. (44), can only be resolved experimentally. However, the canonical problem of 1D permeation, most commonly used to measure permeability under finite deformation, cannot discriminate uniquely between these two forms of constitutive relations and is thus unable to resolve this question. The alternative canonical problem of permeation under torsion, described above, may be able to resolve this question if the flow of interstitial fluid can be visualized experimentally and shown to follow either a rectilinear or helical pattern (Figure

1). In particular, an examination of whether or not the fluid flux pattern follows the deformation according to an affine transformation (Figure 2) may determine the relative contribution of the various terms appearing in the general expression for the permeability tensor, such as in the example given in Eq.(44).

Depending on the material symmetry, the scalar functions $k_i(I_j)$ may depend on a narrower or broader set of strain invariants I_j. In the prior literature, only a dependence on $J=\sqrt{I_3}=\det\mathbf{F}$ has been proposed, as in Eq.(36), motivated in part by the pore closure constraint of Eq.(9). A dependence on other strain invariants would need to be motivated from experimental findings, using testing configurations that can discriminate among the contributions of the various strain invariants. The conceptualization and implementation of such testing configurations may be the subject of future studies.

The orthotropic, transversely isotropic and isotropic strain-dependent formulations presented above model transport properties that exhibit those material symmetries in the reference configuration, but exhibit further anisotropy with applied finite strain. For example, the transversely isotropic model may be applicable to fibrous tissues with a single preferred fiber orientation, such as tendons and some ligaments, or for membranes or sheets with random in-plane fiber orientation. Even if these tissues undergo small strains under normal function, they may still experience large rotations (such as gliding tendons that wrap around bones, ligaments that span across flexing diarthrodial joints, or heart valve leaflets that undergo large bending). The preferred material directions for transport should conform to these large motions, as demonstrated in these formulations.

As a final note, though the presentation of this study focused on the hydraulic permeability tensor, every concept presented here is equally applicable to the diffusivity tensor for solute transport in deformable porous media. Diffusivity is a measure of frictional interactions between the solute and the interstitial solvent and porous solid matrix, just like permeability is a measure of frictional interactions between the interstitial solvent and porous solid. The diffusivity tensor must be symmetric and positive semi-definite according to the same thermodynamic principles leading to these constraints for the permeability tensor (Appendix). Consequently, the same method of formulating constitutive relations based on representation theorems of tensor-valued functions applies.

In summary, this study provided guidelines and formulations for anisotropic strain-dependent transport properties in porous-deformable media undergoing large deformations, such as biological tissues and cells. The general formulation accounted for strain-induced anisotropy. Examples of constitutive relations for isotropic and orthotropic materials were illustrated, though the general framework presented here provides the foundation for any choice of constitutive relations.

Acknowledgments

This study was supported by grants AR46532, AR43628 and AR47369 from the National Institute of Arthritis and Musculoskeletal and Skin Diseases, and GM083925 from the National Institute of General Medical Sciences, of the U.S. National Institutes of Health.

References

1. Basser PJ, Mattiello J, LeBihan D. Estimation of the effective self-diffusion tensor from the NMR spin echo. J Magn Reson B. 1994; 103(3):247–254. [PubMed: 8019776]
2. Basser PJ, Mattiello J, LeBihan D. MR diffusion tensor spectroscopy and imaging. Biophys J. 1994; 66(1):259–267. [PubMed: 8130344]

3. Basser PJ. Inferring microstructural features and the physiological state of tissues from diffusion-weighted images. NMR Biomed. 1995; 8(7–8):333–344. [PubMed: 8739270]
4. Ellegood J, McKay RT, Hanstock CC, Beaulieu C. Anisotropic diffusion of metabolites in peripheral nerve using diffusion weighted magnetic resonance spectroscopy at ultra-high field. J Magn Reson. 2007; 184(1):20–28. [PubMed: 17027305]
5. Hsu EW, Buckley DL, Bui JD, Blackband SJ, Forder JR. Two-component diffusion tensor MRI of isolated perfused hearts. Magn Reson Med. 2001; 45(6):1039–1045. [PubMed: 11378882]
6. Hwang CW, Edelman ER. Arterial ultrastructure influences transport of locally delivered drugs. Circ Res. 2002; 90(7):826–832. [PubMed: 11964377]
7. Jackson A, Yao H, Brown MD, Yong Gu W. Anisotropic ion diffusivity in intervertebral disc: an electrical conductivity approach. Spine. 2006; 31(24):2783–2789. [PubMed: 17108829]
8. Leddy HA, Haider MA, Guilak F. Diffusional anisotropy in collagenous tissues: fluorescence imaging of continuous point photobleaching. Biophys J. 2006; 91(1):311–316. [PubMed: 16603503]
9. Gu WY, Mao XG, Foster RJ, Weidenbaum M, Mow VC, Rawlins BA. The anisotropic hydraulic permeability of human lumbar anulus fibrosus. Influence of age, degeneration, direction, and water content. Spine (Phila Pa 1976). 1999; 24(23):2449–2455. [PubMed: 10626306]
10. Federico S, Herzog W. On the anisotropy and inhomogeneity of permeability in articular cartilage. Biomech Model Mechanobiol. 2008; 7(5):367–378. [PubMed: 17619089]
11. Rivlin RS, Ericksen JL. Stress-deformation relations for isotropic materials. J Rational Mech Anal. 1955; 4:323–425.
12. Liu I-S. On representations of anisotropic invariants. Int J Eng Sci. 1982; 20(10):1099–1109.
13. Bonet, J.; Wood, RD. Nonlinear continuum mechanics for finite element analysis. Cambridge University Press, Cambridge; New York, NY, USA: 1997.
14. Simon BR, Kaufmann MV, McAfee MA, Baldwin AL, Wilson LM. Identification and determination of material properties for porohyperelastic analysis of large arteries. J Biomech Eng. 1998; 120(2):188–194. [PubMed: 10412379]
15. Curnier A, Qi-Chang H, Zysset P. Conewise linear elastic materials. J Elasticity. 1994; 37(1):1–38.
16. Spencer, AJM. Continuum theory of the mechanics of fibre-reinforced composites. Springer-Verlag; Wein, New York: 1984.
17. Noble, B.; Daniel, JW. Applied linear algebra. Prentice Hall; Englewood Cliffs, N.J: 1977.
18. Holmes MH, Mow VC. The nonlinear characteristics of soft gels and hydrated connective tissues in ultrafiltration. J Biomech. 1990; 23(11):1145–1156. [PubMed: 2277049]
19. Lai WM, Mow VC, Roth V. Effects of nonlinear strain-dependent permeability and rate of compression on the stress behavior of articular cartilage. J Biomech Eng. 1981; 103(2):61–66. [PubMed: 7278183]
20. Reynaud B, Quinn TM. Anisotropic hydraulic permeability in compressed articular cartilage. J Biomech. 2006; 39(1):131–137. [PubMed: 16271597]
21. Kohles SS, Roberts JB, Upton ML, Wilson CG, Bonassar LJ, Schlichting AL. Direct perfusion measurements of cancellous bone anisotropic permeability. J Biomech. 2001; 34(9):1197–1202. [PubMed: 11506790]
22. Mansour JM, Mow VC. The permeability of articular cartilage under compressive strain and at high pressures. J Bone Joint Surg Am. 1976; 58(4):509–516. [PubMed: 1270471]
23. Weiss JA, Maakestad BJ. Permeability of human medial collateral ligament in compression transverse to the collagen fiber direction. J Biomech. 2006; 39(2):276–283. [PubMed: 16321629]
24. Ateshian GA, Warden WH, Kim JJ, Grelsamer RP, Mow VC. Finite deformation biphasic material properties of bovine articular cartilage from confined compression experiments. J Biomech. 1997; 30(11–12):1157–1164. [PubMed: 9456384]
25. Iatridis JC, Setton LA, Foster RJ, Rawlins BA, Weidenbaum M, Mow VC. Degeneration affects the anisotropic and nonlinear behaviors of human anulus fibrosus in compression. J Biomech. 1998; 31(6):535–544. [PubMed: 9755038]

26. Klisch SM, Lotz JC. A special theory of biphasic mixtures and experimental results for human annulus fibrosus tested in confined compression. J Biomech Eng. 2000; 122(2):180–188. [PubMed: 10834159]
27. Perie D, Korda D, Iatridis JC. Confined compression experiments on bovine nucleus pulposus and annulus fibrosus: sensitivity of the experiment in the determination of compressive modulus and hydraulic permeability. J Biomech. 2005; 38(11):2164–2171. [PubMed: 16154403]
28. Perie DS, Maclean JJ, Owen JP, Iatridis JC. Correlating material properties with tissue composition in enzymatically digested bovine annulus fibrosus and nucleus pulposus tissue. Ann Biomed Eng. 2006; 34(5):769–777. [PubMed: 16598654]
29. Holmes MH. Finite deformation of soft tissue: analysis of a mixture model in uniaxial compression. J Biomech Eng. 1986; 108(4):372–381. [PubMed: 3795885]
30. Kwan MK, Lai WM, Mow VC. A finite deformation theory for cartilage and other soft hydrated connective tissues--I. Equilibrium results. J Biomech. 1990; 23(2):145–155. [PubMed: 2312519]
31. Suh JK, Spilker RL. Indentation analysis of biphasic articular cartilage: nonlinear phenomena under finite deformation. J Biomech Eng. 1994; 116(1):1–9. [PubMed: 8189703]
32. Almeida ES, Spilker RL. Mixed and Penalty Finite Element Models for the Nonlinear Behavior of Biphasic Soft Tissues in Finite Deformation: Part I - Alternate Formulations. Comput Methods Biomech Biomed Engin. 1997; 1(1):25–46. [PubMed: 11264795]
33. Levenston ME, Frank EH, Grodzinsky AJ. Electrokinetic and poroelastic coupling during finite deformations of charged porous media. J Appl Mech. 1999; 66(2):323–333.
34. Sun DD, Leong KW. A nonlinear hyperelastic mixture theory model for anisotropy, transport, and swelling of annulus fibrosus. Ann Biomed Eng. 2004; 32(1):92–102. [PubMed: 14964725]
35. Garcia JJ, Cortes DH. A nonlinear biphasic viscohyperelastic model for articular cartilage. J Biomech. 2006; 39(16):2991–2998. [PubMed: 16316659]
36. Ateshian GA, Ellis BJ, Weiss JA. Equivalence between short-time biphasic and incompressible elastic material responses. J Biomech Eng. 2007; 129(3):405–412. [PubMed: 17536908]
37. Ehlers W, Karajan N, Markert B. An extended biphasic model for charged hydrated tissues with application to the intervertebral disc. Biomech Model Mechanobiol. 2009; 8(3):233–251. [PubMed: 18661285]
38. Bowen RM. Compressible porous media models by use of the theory of mixtures. Int J Eng Sci. 1982; 20(6):697–735.
39. Ateshian GA. On the theory of reactive mixtures for modeling biological growth. Biomech Model Mechanobiol. 2007; 6(6):423–445. [PubMed: 17206407]
40. Lai WM, Hou JS, Mow VC. A triphasic theory for the swelling and deformation behaviors of articular cartilage. J Biomech Eng. 1991; 113(3):245–258. [PubMed: 1921350]
41. Truesdell, C.; Toupin, R. The classical field theories. In: Flugge, S., editor. Handbuch der Physik. Vol. III/1. Springer-Verlag; Berlin: 1960.
42. Nye, JF. Physical properties of crystals : their representation by tensors and matrices. Oxford University Press; Oxford [Oxfordshire]: 1984.

Appendix

In a mixture of a solid and a fluid, when the effects of viscosity are neglected relative to the effects of frictional interactions between the solid and fluid, under quasi-static conditions and in the absence of external body forces, the momentum equation for the fluid is given by

$$-\phi^f \operatorname{grad} p + \widehat{\mathbf{p}}_d^f = \mathbf{0}, \tag{A1}$$

where $\widehat{\mathbf{p}}_d^f$ is the dissipative part of the internal momentum to the fluid due to frictional interactions with the solid matrix [38–40]. A diffusive drag force $\widehat{\mathbf{p}}_d^s$ also acts on the solid

NIH-PA Author Manuscript

NIH-PA Author Manuscript

matrix. There are two constraints that need to be satisfied by $\widehat{\mathbf{p}}_d^\alpha$ (α=s, f). From the rule of mixtures, which states that a heterogeneous mixture must obey the ordinary equations of a continuum [41], we must have

$$\sum_\alpha \widehat{\mathbf{p}}_d^\alpha = 0 \tag{A2}$$

in the absence of chemical reactions. Furthermore, from the entropy inequality, $\widehat{\mathbf{p}}_d^\alpha$ must satisfy

$$\sum_\alpha \widehat{\mathbf{p}}_d^\alpha \cdot \mathbf{v}^\alpha \le 0, \tag{A3}$$

where $\mathbf{v}^\alpha$ is the velocity of constituent α.

In the absence of chemical reactions, the general form for the diffusive drag that can satisfy (A3) must be

$$\widehat{\mathbf{p}}_d^\alpha = \sum_\beta \mathbf{f}^{\alpha\beta} \cdot (\mathbf{v}^\beta - \mathbf{v}^\alpha), \tag{A4}$$

where $\mathbf{f}^{\alpha\beta}$ ($\alpha \ne \beta$) is the diffusive drag tensor between constituents α and β. In general, $\mathbf{f}^{\alpha\beta}$ may be a function of the strain, temperature, magnitude $|\mathbf{v}^\alpha - \mathbf{v}^\beta|$ of the relative velocities, and fluid content. Equation (A2) can be satisfied for arbitrary velocities, and mixtures of arbitrary pairs of constituents, if and only if

$$\mathbf{f}^{\alpha\beta} = \mathbf{f}^{\beta\alpha}. \tag{A5}$$

Substituting Eq.(A4) into Eq.(A3), recognizing that the dummy indices on the resulting double summation can be interchanged, and making use of Eq.(A5) yields the quadratic form

$$\sum_\alpha \sum_\beta (\mathbf{v}^\beta - \mathbf{v}^\alpha) \cdot \mathbf{f}^{\alpha\beta} \cdot (\mathbf{v}^\beta - \mathbf{v}^\alpha) \ge 0. \tag{A6}$$

Therefore, the entropy inequality implies that the tensor $\mathbf{f}^{\alpha\beta}$ must be positive semi-definite (its eigenvalues must be non-negative [17]). An interesting property of the quadratic form of Eq.(A6) is that it places a constraint only on the symmetric part of $\mathbf{f}^{\alpha\beta}$. This is easily shown by splitting $\mathbf{f}^{\alpha\beta}$ into the sum of its symmetric and antisymmetric parts, and recognizing that the quadratic form of the latter reduces to zero. It follows that this antisymmetric part has no influence on the energy dissipated by this frictional interaction, represented by the term on the left-hand-side of Eq.(A6); consequently, it is *not* observable [42]. On the basis of this argument, $\mathbf{f}^{\alpha\beta}$ is taken to be symmetric, $(\mathbf{f}^{\alpha\beta})^T = \mathbf{f}^{\alpha\beta}$, since it can never be shown to be otherwise.

In the case of a solid-fluid mixture, the diffusive drag tensor $\mathbf{f}^{fs}$ may be related to the spatial hydraulic permeability tensor **k** via $\mathbf{f}^{fs} = (\phi^f)^2\mathbf{K}^{-1}$, so that $\widehat{\mathbf{p}}_d^f = -\phi^f \mathbf{k}^{-1} \cdot \mathbf{w}$, where $\mathbf{w} = \phi^f(\mathbf{v}^f - \mathbf{v}^s)$ is the flux of interstitial fluid relative to the solid. Substituting this relation for $\widehat{\mathbf{p}}_d^f$ into Eq.(A1) produces Darcy's law, as presented in Eq.(1). A symmetric, positive semi-definite $\mathbf{f}^{fs}$ implies the same properties for **k**.

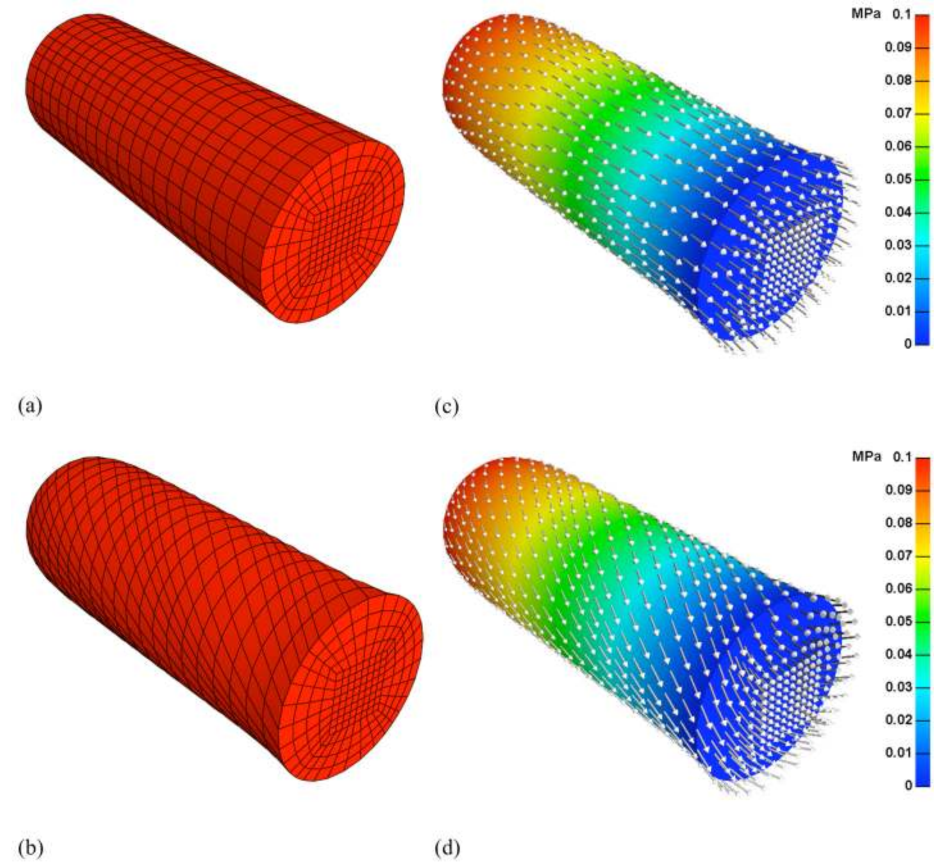

Figure 1.
Finite element results for permeation through a cylinder subjected to finite torsion. (a) Cylinder geometry in reference configuration. (b) Cylinder geometry after one half-turn (180°) twist. (c) Vector plot of relative volume flux of solvent in deformed configuration, using $\mathbf{k} = k_0\mathbf{I}$, which does not account for strain-induced anisotropy. (d) Vector plot of flux in deformed configuration, using $\mathbf{k} = k_1\mathbf{b}$, which accounts for strain-induced anisotropy.

NIH-PA Author Manuscript
NIH-PA Author Manuscript

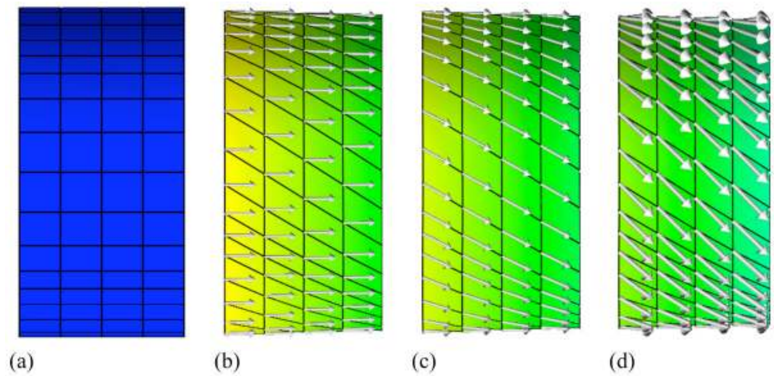

Figure 2.

Close-up of relative volume flux of solvent, in relation to mesh deformation: (a) Reference configuration. (b) $\mathbf{k} = k_0\mathbf{I}$. (c) $\mathbf{k} = k_1\mathbf{b}$. (d) $\mathbf{k} = 2k_2\mathbf{b}^2$. Case (c) confirms that this constitutive relation produces strain-induced anisotropy that follows an affine transformation of preferred material directions, since the flux realigns exactly with the deforming mesh. Cases (b) and (d) represent non-affine transformations.